

Conclusive Evidence for Internal Dielectric Charging Anomalies on Geosynchronous Communications Spacecraft

Gordon L. Wrenn*

DRA Farnborough, Hampshire GU14 6TD, England, United Kingdom

When the ANIK E1 and E2 communications spacecraft suffered serious failures of their momentum wheel control systems, it was postulated that the satellites were subjected to bulk (internal dielectric) charging followed by discharge that disabled key circuitry. This paper effectively confirms the hypothesis by linking the events to a well-established pattern of operational anomalies on another spacecraft. Since March 1991, a commercial geosynchronous satellite has experienced over 50 specific, but relatively trivial, mode switches. These are analyzed in relation to energetic electron fluences measured at GOES-7 and METEOSAT-3; without exception they coincide with periods of relatively high flux. Combining the measurements, the critical directed energy fluence is calculated to be $1 \times 10^{11} \text{ MeV cm}^{-2}$. This figure is consistent with the theoretical breakdown threshold and CRRES data characterizing the discharge process; it fits with an effective shielding thickness of less than 0.2 mm of aluminum. Three switches in the days preceding the ANIK failures strongly argue for a common explanation, although it may be impossible to even identify actual discharge sites. Modern communications spacecraft employ tried and tested techniques for electrostatic discharge protection, but it is clear that the recognized hazard of internal dielectric charging has often been underestimated and shielding guidelines overlooked.

Nomenclature

E	= electron energy, MeV
E_0	= e-folding energy, MeV
E_C	= lower cut-off energy, MeV
J	= electron fluence (flux \times time), $\text{cm}^{-2} \text{ sr}^{-1} \text{ MeV}^{-1}$
J_0	= total electron fluence, $\text{cm}^{-2} \text{ sr}^{-1}$
J_C	= net fluence with energy $> E_C$, $\text{cm}^{-2} \text{ sr}^{-1}$
T_0	= total energy fluence, MeV cm^{-2}
πJ_0	= total directed fluence, cm^{-2}

Introduction

ON January 20, 1994, the \$300 million Telesat Canada communication satellites, ANIK E1 and E2, both failed because of problems with their momentum wheel control systems. E1 was out of service for just a few hours, but the recovery of E2 will take many months, and the cost of rescue, lost revenue, and reduced lifetimes is put at tens of millions of dollars.^{1,2} Expert opinion is that "it is likely that the satellites which failed were subjected to bulk charging followed by a discharge that disabled key circuitry."¹ It is the objective of this paper, by detailing the analysis of a series of relatively trivial but persistent anomalies on another geosynchronous communications satellite, here referred to as DRA δ , to elevate likely to virtually certain.

Since instrumented satellites were first launched, few have operated in exactly the way intended for very long. Given the high cost and long lead time for deploying systems in space, dedicated build-and-test technologies have been developed in an attempt to increase the reliability and lifetime of every component. Accepting that mass and power are always at a premium, there is only a limited scope for built-in redundancy; however, essential miniaturization has yielded some intrinsic enhancement in reliability. The adoption of proven design methods with careful component selection and rigorous qualification testing (e.g., vibration and thermal cycling in vacuum) have generally achieved high standards, but it has been impossible to eliminate what have become classified as operational anomalies.

Such a catch-all term, operational anomalies, obviously encompasses a whole range of nonconformance events, and it is helpful to consider the possible locations within the mission segments partitioned as follows:

- 1) ground control facility with equipment, both hardware and software, as well as human processes,
- 2) communications with associated telemetry and telecommand problems, and
- 3) spacecraft, including the platform with onboard data-handling and payload instrumentation.

The majority of problems are probably associated with ground control, communications, and the human interface (most likely involving human input to a computer interface). Assuming that all internal interferences have been eliminated, anomalies originating in the spacecraft, subsequent to launch and injection, can be regarded as environmental in that they are a consequence of the operating conditions found in orbit. The following list of such hazards and effects might, depending upon orbit, have to be addressed at the design stage:

- 1) Thermal strain \rightarrow part or system fatigue.
- 2) Highly ionising radiation dose \rightarrow part or system fatigue.
- 3) Highly ionising radiation burst \rightarrow single-event upset or latchup.
- 4) Electrostatic charging \rightarrow electrostatic discharge (ESD).
- 5) Electromagnetic pulse \rightarrow current and voltage transients.
- 6) Ultraviolet, atomic oxygen \rightarrow surface corrosion.
- 7) Micrometeoroids, space debris \rightarrow impact damage.
- 8) Ionospheric irregularities \rightarrow scintillations, range errors.
- 9) radio-frequency signals \rightarrow interference, noise.

Such threats to the spacecraft segment are particularly serious because there is often little that can be done to overcome problems once the hardware is in orbit. In geosynchronous Earth orbit (GEO), the tenuous plasma environment is frequently well suited to the support of spacecraft surface electrostatic charging,^{3,4} and this makes proper ESD protection particularly important for such missions. Many technical papers and satellite design standards have focused on the electric potential developed at the satellite surfaces immersed in the plasma environment.^{5,6} Key lessons were learned in the late 1970s and early 1980s, as successful protection techniques were developed to alleviate and effectively eliminate problems associated with surface charging. However, operational anomalies have obviously not been eliminated, and bulk charging has now been recognized as a significant source of ESD aboard well-designed satellites such as ANIK.⁷⁻⁹ Given a one-off or a few-off failure scenario, it is

Received Oct. 20, 1993; revision received March 18, 1994; accepted for publication June 2, 1994. Copyright © 1994 by the British Crown. Published by the American Institute of Aeronautics and Astronautics, Inc., with permission of the Controller of Her Britannic Majesty's Stationery Office.

*Section Leader, Spacecraft Environment and Protection, Space Technology Division, Space and Communications Department, Q134.

impossible to prove causality with any of the environmental interactions listed above. This paper establishes a link with a pattern of similar anomalies, using apposite measurements of energetic electrons in GEO, to introduce statistical significance into the applied logic, and thereby provides some conclusive evidence that internal dielectric charging was indeed the culprit in the ANIK crime.

Operational Anomalies

Traditionally, satellite mission managers have been reticent about reporting recorded anomalies, but in recent years attitudes have changed. Once it was realized that the space environment could somehow be blamed for some of their problems, there was a tendency to seek such an explanation for every out-of-limits signal, even though this belied any acknowledgment of inadequacies in protection design. The National Geophysical Data Center at Boulder initiated a database of declared environmental anomalies¹⁰ so that open reporting might eventually permit a comprehensive analysis of space weather effects and enable cost-effective protection strategies to be employed.

It is virtually impossible to obtain proof of the cause of a single anomaly, but, given a series of like anomalies, it is often possible to identify a pattern that can be compared with available environmental monitors to establish a plausible cause and effect. This is particularly true for GEO missions, where the altitude, latitude, and longitude of the spacecraft remain constant. Since there is a scarcity of environment monitors that are reliable and available in near-real time, it is often necessary to count on indirect evidence from solar and geomagnetic indices and statistical arguments. An excellent example of this procedure was presented by the case of MARECS-A, on which the electrostatic charging of surface elements frequently triggers discharges, causing a number of specific switching anomalies.^{6,11} The pattern of occurrence, which peaks between local midnight and dawn, matches that of plasmasheet electrons injected from the magnetotail and drifting eastward in the geomagnetic field; the events also correlate with substorms, being reflected by indices of geomagnetic activity such as local or planetary a and K values.¹² The consequent understanding of the problem has permitted its reduction on the ensuing line of European communications spacecraft embracing MARECS-B2, ECS-1, ECS-2, ECS-4, and ECS-5.

Since photoelectron emission in sunlight prevents surface charging, the occurrence of such anomalies in sunlight should be relatively rare. However, Wrenn and Sims⁴ analyzed 1464 GEO anomalies, listed in the NGDC database, in relation to geomagnetic activity and showed that the classic local time pattern only exists during the active periods; at quieter times, anomalies are evenly distributed throughout the day as presented in Table 1. These results clearly show that only a minority of the events, those during infrequent geomagnetically disturbed periods, fit the surface charging pattern with respect to both local time and geomagnetic activity. In general, the types of anomaly (monitoring-bit errors, spurious status switching, and mode changes) are similar to those that have been assigned to surface charging effects. Some of these events might be due to single-event upsets caused by cosmic rays, but it has long been suspected that many result from internal dielectric charging with consequent ESD.

Internal Dielectric Charging

Internal dielectric (bulk, buried, or deep) charging (IDC) was postulated as a spacecraft hazard in the 1970s¹³; confirmation and

understanding of the phenomenon has since been sought in data from the laboratory and satellites.^{7,9,14} The theory is that high-energy electrons, incident upon a thick dielectric, can produce a buildup of embedded charge, which induces large potential differences through the material. Such buildup requires the rate of charge deposition to exceed the rate of leakage due to the small but finite conductivity of the dielectric. Given a sustained flux of high-energy electrons, the potential gradient can exceed a breakdown threshold for the material, when a discharge will be triggered. The term internal dielectric charging is now used in recognition that the charging site may be shallow or may be an embedded floating conductor. It has been demonstrated that both coaxial cables¹⁵ and printed circuit boards (PCBs)¹⁶ can be made to break down when irradiated with electron beams.

However, it had been extremely difficult to get conclusive in-flight evidence for the phenomenon, since few convincing data sets existed.^{7,17} The morphology of MeV electrons seen at GEO had been described.¹⁸ Since the temporal variability is complex, it was difficult to derive a meaningful model with respect to an available index¹⁹ and suitable data from orbiting detectors were seldom accessible. Seven star-sensor shutter anomalies, which occurred in the Air Force Defense Support Program during 1980–1982 after several trouble-free years, correlated with >1.2 -MeV electron enhancements.⁷ The source of numerous anomalies on METEOSAT satellites had been diligently pursued,^{20,21} but the likely role of internal charging appeared to be masked by a multiplicity of effects. The same was largely true for reported upsets on TDRS satellites.²²

Some evidence of bulk discharge was obtained from SCATHA,¹⁷ but it is the recent results from the Combined Release and Radiation Effects Spacecraft (CRRES), in respect of observing both the outer-zone electrons²³ and internal discharges²⁴ and also establishing correlations with onboard anomalies,²⁵ that have dramatically changed the picture. The Internal Discharge Experiment (IDM) detected 4300 pulses during the 14-month mission; it determined the susceptibility of different dielectric samples and configurations, detected an aging effect on extended exposure to radiation, and established a leakage time constant that controls the rate of multiple pulsing.²⁴ It has been possible to create a quasistatic model of the outer-zone electrons, based upon the readily available geomagnetic activity index A_p , and to show that this is much more representative than previous static models.²³ CRRES exhibited eight different types of anomaly in geosynchronous transfer orbit, 674 in all, and most of these correlated well with high electron energy flux.²⁵ It should be noted that the great majority of these anomalies occurred at altitudes well inside $6.6R_E$ (GEO). However, this evidence from CRRES does leave a small credibility gap, because CRRES, like SCATHA, was effectively a test-bed for charging studies. It was not typical of operational communications satellites, which mostly have a conservative design with respect to charge alleviation and ESD protection; it is also acknowledged that the larger radiation doses experienced in GTO significantly aggravate the problem.

GOES-7, at 108 deg W, carries a detector that gives integrated fluxes of electrons with energy greater than 2 MeV [data supplied by Space Environment Services Center (SESC); the detector is sensitive to very energetic protons, and thus the data become ambiguous at times of solar proton events]. Plots of 5-min averages and tables of daily fluences are published weekly by the NOAA SESC at Boulder. For each week of the three years 1991–1993, Fig. 1 records the spread between minimum and maximum daily fluence ($\text{cm}^{-2} \text{sr}^{-1}$). The large range of variation does not simply follow any solar cycle index; extreme values were centered on March 28, 1991 (6.8×10^9); May 12, 1992 (5.5×10^9); September 6, 1992 (2.3×10^9); October 2, 1992 (3.5×10^9); and August 21, 1993 (2.1×10^9). Note that January 1994 did not reach such heights.

METEOSAT-3, located between 40 and 70 deg W, carries an electron spectrometer for energies above 43 keV; the top channel has no discrete high-level discriminator and therefore effectively measures the integrated flux above 0.2 MeV [instrument built by Los Alamos National Laboratory (LANL), data supplied by University College London²¹]. Figure 2 shows diurnal profiles of these fluxes 1) averaged over a month (August 1992) and 2) from a selected disturbed day June 7, 1993. The pattern of variation reflects the asymmetry in the geomagnetic field controlling the outer Van Allen belt, yielding

Table 1 Analysis of GEO anomalies recorded in NGDC database

	Local time range		
	00–24 (24 h)	23–09 (10 h)	09–23 (14 h)
Very quiet (least active 10%)	54	26	28
Quiet (next 15%)	86	38	48
Normal (middle 50%)	640	322	318
Active (next 15%)	308	161	147
Very active (most active 10%)	376	248	128
Totals	1464	795	669

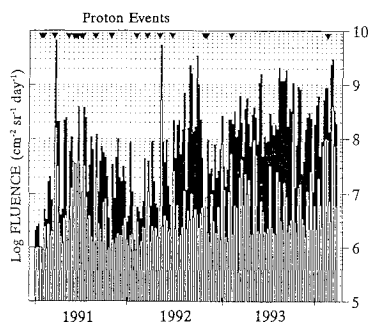


Fig. 1 Daily fluence of >2-MeV electrons measured at GOES-7; solid bars cover the range between minimum and maximum values for each week during 1991–1993. The identified proton events cover temporary data losses.

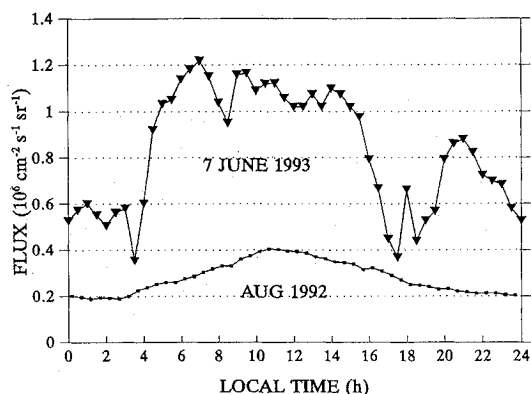


Fig. 2 Diurnal variation of >2-MeV electron flux measured at METEOSAT-3: monthly means for August 1992 and a typical disturbed day, June 7, 1993.

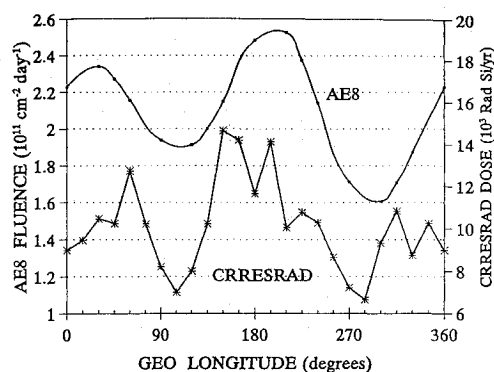


Fig. 3 Daily fluence and annual dose of energetic electrons, plotted as a function of satellite longitude, using AE8 and CRRESRAD models for $6.6R_E$.

a factor-of-2 enhancement for midday compared to midnight. The diurnal variation at higher energy is greater; the GOES-7 measurements typically exhibit a factor of 10. The reason for this is twofold: the higher-energy electrons are less tightly trapped, and the lower-energy detection includes a component of the plasmasheet population, which has a very different distribution.⁴ The spectrometer was switched off during March and April 1991.

When combining data from satellites at different longitudes, it must be appreciated that the field asymmetry again introduces some variation both in the magnetic L shell and in the displacement from the geomagnetic equator. The latter gives a reduction in incident flux because electrons with large pitch angle mirror close to the equator; any inclination of orbit is also an important consideration in this regard. In Fig. 3 the AE8 model of outer-zone electrons (>0.5 MeV) is used to plot the mean flux as a function of satellite longitude in GEO; although this model is known to be deficient, the inferred factor-of-2 variation should be representative. Also plotted

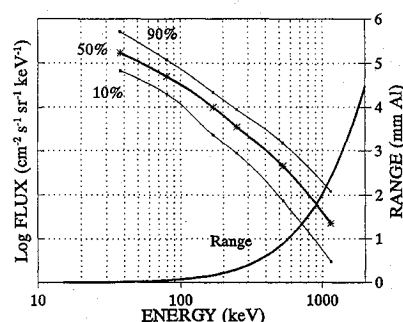


Fig. 4 Flux of GEO electrons averaged over all local times (1977–1978), and range of electrons in aluminum, both as functions of energy.

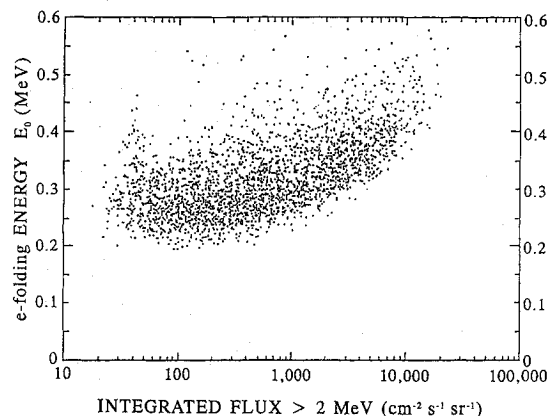


Fig. 5 Characteristic relationship between e-folding energy and >2-MeV integrated flux for electrons measured in GEO: scatterplot of over 2000 data points.²⁸

are dose values from the empirical CRRESRAD model²³ (Lolet, >1 MeV electrons, high activity) for GEO; these essentially support the factor-of-2 conclusion.

Given an integrated fluence of electrons incident upon a satellite, the charge deposited in a particular slab of dielectric will depend upon the thickness of shielding above it and the energy spectrum of the electrons. Typically, breakdown of the dielectric can occur when the internal electric field exceeds 2×10^5 V/cm. Wenaas et al.¹⁶ reported that a deposited charge of 5×10^{11} e/cm² will produce breakdown of a PCB in the absence of excess leakage. The finite conductivity of all dielectrics will permit some leakage, but if it is sufficiently small, the charge buildup can take place over many hours, possibly a day or two. Figure 4 shows the electron range in millimeters of aluminum as a function of energy²⁶ and also shows mean energy spectra measured by Baker et al.²⁷ for all local times during 1977–1978; the 10% and 90% probability-level contours give some idea of the range of variation but do not reflect extreme enhancements. Figure 5 is a scatterplot of some 2000 GEO measurements, which show that there is indeed a trend for the characteristic energy E_0 to increase with integrated flux.²⁸ It is clear that the energy distribution of the incident electrons will be a critical factor. However, Vampola⁷ concluded that “the combination of maximum expected electron fluxes and the small energy associated with the bulk dielectric breakdown permits the elimination of bulk charging as a spacecraft problem through minimal shielding, 400 mg/cm² (≈ 1.5 mm Al), of all cables and circuit boards otherwise exposed to the environment, and through desensitizing digital logic inputs which are serviced by cables.”

Attitude Sensor Anomalies on DRA δ

Since March 1991, a commercial geosynchronous communications spacecraft, here called DRA δ , has suffered many spurious mode switches by way of attitude-sensor disable anomalies; these occurred on the dates and Universal Times given in Table 2. At each anomaly, two telemetry channels changed state to indicate a

Table 2 Two-day fluences on anomaly days: March 1991–March 1994

No	Date	UT, hh:mm	Fluence		E_0 , MeV	πJ_0 , 10^{11} cm^{-2}	πT_0 , $10^{11} \text{ MeV cm}^{-2}$
			>2 MeV, $10^6 \text{ cm}^{-2} \text{ sr}^{-1}$	>0.2 MeV, $10^9 \text{ cm}^{-2} \text{ sr}^{-1}$			
1	28 Mar 91	13:49	7430	—	—	—	—
2	30 Mar 91	09:55	8200	—	—	—	—
3	12 May 92	13:29	7100	195	0.54	8.8	4.8
4	15 May 92	08:43	1820	82	0.47	3.9	1.9
5	25 July 92	13:27	273	63	0.33	3.6	1.2
6	13 Aug 92	11:51	1180	96	0.41	4.9	2.0
7	05 Sep 92	11:51	2070	119	0.44	5.8	2.6
8	07 Sep 92	12:03	3900	113	0.53	5.1	2.7
9	20 Sep 92	10:43	217	72	0.31	4.3	1.3
10	02 Oct 92	03:53	5000	159	0.52	7.3	3.8
11	03 Oct 92	10:25	6900	167	0.56	7.4	4.2
12	17 Oct 92	10:28	260	81	0.31	4.8	1.5
13	15 Nov 92	12:19	116	81	0.27	5.2	1.4
14	13 Dec 92	11:50	123	75	0.28	4.8	1.3
15	05 Jan 93	10:30	460	133	0.32	7.8	2.5
16	08 Jan 93	13:26	370	116	0.31	6.9	2.1
17	03 Feb 93	09:18	440	101	0.33	5.8	1.9
18	11 Feb 93	09:46	420	108	0.32	6.2	2.0
19	24 Feb 93	13:24	540	96	0.35	5.3	1.9
20	18 Mar 93	11:05	660	95	0.36	5.2	1.9
21	26 Mar 93	10:49	220	75	0.31	4.5	1.4
22	11 Apr 93	10:54	610	83	0.37	4.5	1.6
23	22 Apr 93	11:10	330	65	0.34	3.6	1.2
24	21 May 93	08:08	390	78	0.34	4.4	1.5
25	07 June 93	05:17	2500	126	0.46	6.1	2.8
26	09 June 93	09:11	2600	111	0.48	5.3	2.5
27	14 July 93	08:51	560	86	0.36	4.7	1.7
28	18 Aug 93	17:08	1080	92	0.40	4.7	1.9
29	20 Aug 93	22:21	3300	118	0.50	5.5	2.8
30	23 Aug 93	11:20	3300	62	0.61	2.7	1.6
31	05 Sep 93	12:29	1500	117	0.41	5.9	2.5
32	08 Sep 93	12:12	1010	60	0.44	3.0	1.3
33	15 Sep 93	07:34	2700	116	0.48	5.5	2.6
34	18 Sep 93	14:16	3600	67	0.62	2.9	1.8
35	03 Oct 93	08:51	670	92	0.37	5.0	1.8
36	11 Oct 93	10:22	1190	140	0.38	7.4	2.8
37	13 Oct 93	04:56	1580	123	0.41	6.2	2.6
38	16 Oct 93	08:31	1000	68	0.43	3.4	1.4
39	06 Nov 93	09:19	660	147	0.33	8.4	2.8
40	08 Nov 93	08:52	1750	152	0.40	7.8	3.1
41	10 Nov 93	12:36	1030	83	0.41	4.2	1.7
42	04 Dec 93	11:09	260	127	0.29	7.9	2.3
43	07 Dec 93	11:58	350	91	0.32	5.3	1.7
44	19 Dec 93	08:24	460	136	0.32	8.0	2.5
45	23 Dec 93	10:15	213	85	0.30	5.2	1.6
46	14 Jan 94	10:36	351	121	0.31	7.2	2.2
47	16 Jan 94	12:40	790	143	0.35	8.0	2.8
48	19 Jan 94	08:15	540	151	0.32	8.8	2.8
49	09 Feb 94	08:17	720	148	0.34	8.3	2.8
50	16 Feb 94	10:17	1420	122	0.40	6.3	2.5
51	23 Feb 94	04:08	—	131	—	—	—
52	25 Feb 94	06:41	1130	100	0.40	5.1	2.1
53	10 Mar 94	08:34	3300	166	0.46	8.0	3.7
54	12 Mar 94	08:55	4700	155	0.51	7.1	3.7
55	15 Mar 94	09:50	3200	127	0.49	6.0	2.9
56	17 Mar 94	11:38	4700	134	0.54	6.1	3.3
57	25 Mar 94	09:17	630	85	0.37	4.6	1.7
Nonanomaly days			90	35	0.30	2.1	0.6

resetting of particular latches, effectively removing the failure protection logic on the IRES units until re-enable commands were sent (a few minutes only). The two relays are supplied by a common 5-V line, and the switchings imply a transient undervoltage detection, presumably produced by a noise spike generated by the ESD. It is possible to determine the probable entry point of the noise spike within the attitude measurement equipment (AME) circuit board, but much more difficult to locate the source of the discharge. A detailed circuit analysis is beyond the scope of this paper; it has been addressed elsewhere, and appropriate changes were made to a follow-on mission, DRA ϵ , to achieve a successful desensitization.

The first two upsets in March 1991 occurred 5 to 7 days after a large solar proton event and during a rare and dramatic injection of MeV electrons into the magnetosphere.²⁹ Figure 6 shows hourly averages of the GOES-7 flux and the accumulated fluence through the interval. An assumed background of $1100 \text{ cm}^{-2} \text{ s}^{-1} \text{ sr}^{-1}$ has been subtracted from all measurements. The peak flux is

$$1.4 \times 10^5 \text{ cm}^{-2} \text{ s}^{-1} \text{ sr}^{-1}$$

and the final fluence is

$$1.55 \times 10^{10} \text{ cm}^{-2} \text{ sr}^{-1}$$

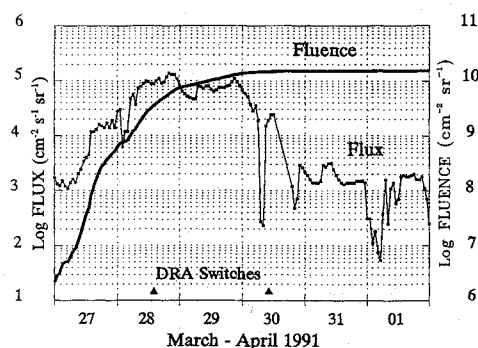


Fig. 6 Flux and fluence of >2-MeV electrons measured at GOES-7 during 6 days in March–April 1991; times for the first two DRA δ AME switches are shown.

For charge deposition in a thin layer, the directed fluence is calculated by assuming an effective solid angle of π sr. At upset 1, the directed fluence equates to

$$1.1 \times 10^{10} \text{ cm}^{-2}$$

and at upset 2,

$$4.6 \times 10^{10} \text{ cm}^{-2}$$

for a change of

$$3.5 \times 10^{10} \text{ cm}^{-2}$$

These data, taken with those for later periods of very high flux, suggest that at the time of an anomaly, the stored charge is dissipated and another buildup commences (after upset 1, the circuits were re-enabled at 14:11); the difference between 1.1×10^{10} for upset 1 and 3.5×10^{10} for upset 2 is not surprising, because it is clear that the GOES-7 measurements can only be a coarse yardstick for the interaction, the separation of the spacecraft being close to 6 h in local time. However, CRRES data have demonstrated that the contribution of multiple sites and partial discharge cannot be discounted.²⁴

Given the fluence for energies >2 MeV, it is necessary to calculate the total fluence over all energies. For this, a spectral shape has to be assumed, and following Koons and Gorney,¹⁷ the following equation is used for the differential number fluence:

$$\frac{dJ}{dE} = \frac{J_0}{E_0} \exp\left(-\frac{E}{E_0}\right) \quad (1)$$

It then follows that for the net fluence, $E > E_C$, we have

$$J_C = J_0 \exp(-E_C/E_0) \quad (2)$$

where E_0 is the characteristic e-folding energy and E_C is the lower cutoff energy. The total energy fluence is

$$T_0 = J_0 E_0 \quad (3)$$

To date, over 50 more DRA δ AME anomalies have occurred between May 12, 1992, and March 31, 1994. Figures 7 and 8 show how the dates relate to the variation of 2-day electron fluence as measured by GOES-7 and METEOSAT-3; the geomagnetic index A_p (provisional values supplied by SESC) is also plotted. The 2-day integration was adopted after noting the minimum interval between events; it also overcomes sampling problems, given that the available daily fluences from the satellites are separated in local time. For each day the measured fluence is taken with addition of that for the previous day, giving the values listed in Table 2 for the anomaly days. There is a striking coincidence between anomaly occurrence and enhanced fluence.

Combination of the GOES-7 and METEOSAT-3 data, with the assumption of Eq. (1), permits the calculation of both the characteristic energy E_0 and the total directed fluence πJ_0 for each of the

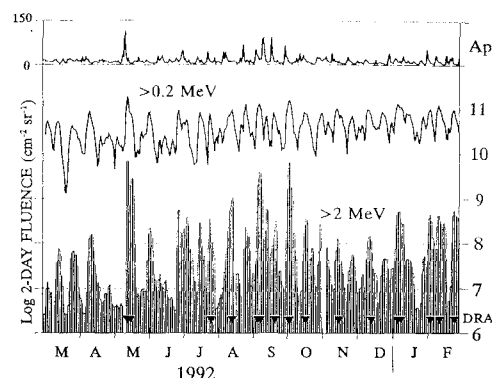


Fig. 7 Two-day fluence of electrons measured at GOES-7 and METEOSAT-3 during March 1992–February 1993. Geomagnetic A_p and dates of DRA δ AME switches are also shown.

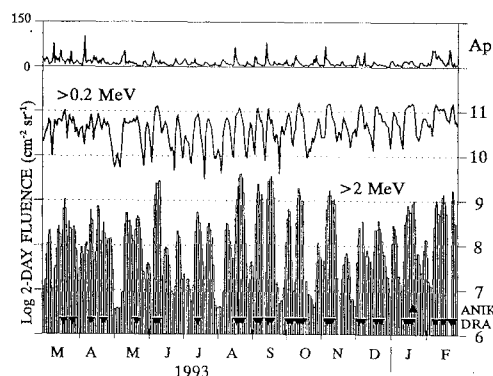


Fig. 8 Two-day fluence of electrons measured at GOES-7 and METEOSAT-3 during March 1993–February 1994. Geomagnetic A_p and dates of DRA δ AME switches and ANIK failures are also shown.

events; these are also listed in Table 2. The resulting values of E_0 cover a significant range, but they fit with previous measurements and generally support the observed pattern of spectral hardening associated with intensification²⁸; this gives considerable confidence in the calibration of both detectors. Removing all days immediately prior to anomalies from the 2-year data set, and averaging the 2-day fluences, gives $9 \times 10^7 \text{ cm}^{-1} \text{ sr}^{-1}$ for GOES-7 and $3.5 \times 10^{10} \text{ cm}^{-2} \text{ sr}^{-1}$ for METEOSAT-3; this corresponds with a directed fluence of $2.2 \times 10^{11} \text{ cm}^{-2}$ with an e-folding energy of 0.3 MeV. It is not possible to verify the spectral assumption; alternative power-law functions have been fitted to outer-zone electrons,²⁴ but the calculated values of J_0 and E_0 should adequately reflect the relative intensity and hardness of the incident fluxes. Note that most of the listed fluence values exceed $3 \times 10^{11} \text{ cm}^{-2}$; given the uncertainties in the combined data and the calculations, one could not expect an absolute accuracy better than a factor of about 4.

In every case, the particle data support the proposition that, at the time of an anomaly, the recent fluence of energetic electrons is above some threshold required for internal charging to induce a breakdown in a dielectric. Inspection of the table hints that the threshold could reflect either a rise in current or spectral hardening. Taking into account the spacings between the spacecraft and the fact that the threshold fluence is time-dependent (because of the leakage factor), the correlation is remarkable. The final column in Table 2 lists the total directed energy fluence ($\pi T_0 = \pi J_0 \cdot E_0$) which seems to be a better threshold indicator; the values are a factor of 2 above the equivalent figure for nonanomaly days, $0.6 \times 10^{11} \text{ MeV cm}^{-2}$. IDM data from CRRES indicates a flux threshold for pulsing of $(1 \text{ to } 5) \times 10^5 \text{ e cm}^{-2} \text{ s}^{-1}$; this translates to 2×10^{10} to 10^{11} cm^{-2} in 2 days,²⁴ which is in good agreement. However, the threshold fluence must be a function of the discharge site geometry, area, and configuration as well as the properties of the dielectric. The quantitative agreement must be partly fortuitous; it suffices to claim that there are no inconsistencies between these data and the CRRES observations.

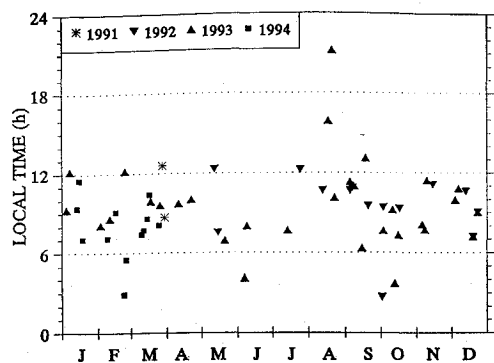


Fig. 9 Distribution of DRA δ AME switches in relation to local time and season.

Any doubts that the anomalies are due to internal dielectric charging can be further dispelled by looking at their distribution in local time and season. Figure 9 shows that there is no tendency for events to occur in the midnight-to-dawn sector, or near equinox, as expected for surface charging effects.⁴ However, the distribution in local time is not fully explained by the profiles of Fig. 2, given the long charging times.

Discussion

Having shown that energetic electron fluences were sufficiently large to produce ESD and trigger the anomalies, a key question relates to where the charge-discharge site (or set of sites) is located. Clearly, it must be close to the surface of the spacecraft, where any effective shielding is small. It is possible to model the electron transport using a Monte Carlo computer code such as CYLTRAN³⁰ to determine the charge deposited for unit fluence, as a function of shielding thickness, for a defined energy spectrum. Assuming the distribution of Eq. (1), setting $E_0 = 0.25$ MeV and then 0.6 MeV to cover the measured range of values gives the result plotted as Fig. 10. In each case, the total fluence required to produce a charge deposition of 3×10^{11} e/cm² is calculated with respect to a shielding thickness in millimeters of aluminum. Taking the total directed fluence (πJ_0) and E_0 figures from Table 2, it appears that, for charge deposition to exceed the 3×10^{11} -e/cm² threshold, the shielding thickness of the dielectric discharge site must have been very small—less than ≈ 0.2 mm of aluminum. Thermal blankets contribute less than this, but the spacecraft structure is considerably thicker. Assuming that there are no PCBs outside the structure, coaxial cables become the prime candidates, particularly those that are linked to the 5-V line and the sensitive circuits by any available conduction path.

Although the actual AME anomalies present no threat to the DRA δ mission, they do present an annoyance to operations staff and raise some disquiet. Their frequency may rise either because of increased activity in the energetic electron environment (Fig. 1 gives few clues to what the future holds, but there is evidence that fluences peak towards solar minimum³¹) or because of an increase in discharge susceptibility; ESD often produces tracking, which raises the probability of subsequent discharges. However, the frequency of observable effects may then be higher or lower because, although the number of current spikes might rise, their amplitude might decrease below a damage threshold.

A study of Figs. 7 and 8 suggests that the susceptibility has indeed increased since the first four switchings in March 1991 and May 1992. A GOES-7 flux of about 10^8 cm⁻² sr⁻¹ day⁻¹ now appears sufficient to trigger the ESD, rather than a few times 10^9 cm⁻² sr⁻¹ day⁻¹; in 1991 there were many days with flux above 10^8 cm⁻² sr⁻¹ day⁻¹ that caused no problems. Again, this is in agreement with the CRRES IDM findings.²⁴ Higher susceptibility could result from a change in fluence threshold or in leakage time constant; extended radiation exposure is unlikely to be a factor in GEO. If the threshold could fall much below the 10^8 -cm⁻² level, it seems likely that the phenomenon would have been more in evidence over last two decades.

Enhancements of energetic electrons often do follow geomagnetically disturbed periods, with a lag of a few days, but study of

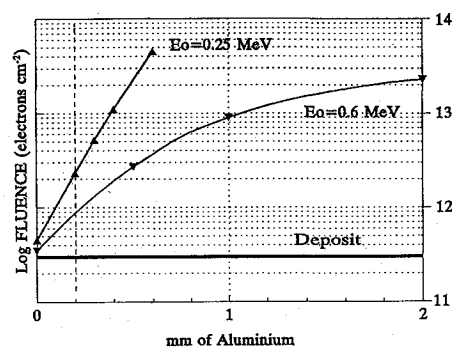


Fig. 10 Fluence required to deposit 3×10^{11} e cm⁻², plotted as a function of shielding thickness for two e-folding energies, 0.25 and 0.6 MeV.

the plots of provisional A_p in Figs 7 and 8 suggests that this could be very much a hit-or-miss rule for prediction purposes. Koons and Gorney¹⁹ and Brautigam et al.²³ have made considerable strides, but are some way from accurate forecasting. Since internal charging is a slow process, any requirement for circumvention, in the absence of an onboard monitor, would best be served by arranging access to GEO electron data in near-real time.

AME anomalies have also been logged on DRA α with the same platform design, on October 2, 1992, at 13:42 and May 3, 1993, at 00:47, coinciding with fluence peaks. A number of automatic reconfiguration mode (ARM) switchings have been reported on ECS-2 (22JUL91, 13MAY92, 19AUG93) and ECS-4 (25MAR90, 28MAR91, 18JUL91, 12MAY92, 13AUG92, 13JAN93, 14JUL93, 05SEP93) (Derbyshire, ESTEC, private communication). Reference to the GOES-7 data for these dates suggests that IDC was probably responsible for most, if not all, of these anomalies.

The week of the January 12–20, 1994, was an extended interval of enhanced electron flux, although the peaks in daily fluence were lower than on previous days; calculated E_0 values (boldface dates in Table 2) indicate a relatively soft spectrum. It can be speculated that the ANIK failures occurred then because 1) they required the charge buildup over some 6 days, 2) the unusual electron energy distribution matched a particular discharge susceptibility, or 3) an aging process had critically increased susceptibility by that date. Each of these options, or any combination, heralds some disconcerting reservations about the future operations of E1.

Conclusions

In spite of all the precautions taken to avoid charging effects on the particular platform, 57 AME switches have occurred on DRA δ to date. These anomalies are undoubtedly due to ESD, resulting from internal dielectric charging. The excellent correlation of the switching events with electron measurements at GEO gives the first real statistical evidence for IDC on a fully protected applications spacecraft. The fact that other satellites, with apparently identical platforms, have been free from these problems highlights the lack of understanding that hinders discharge-site identification and therefore erodes confidence in some of the tried and tested ESD protection measures.

It is important to appreciate that the internal charging process contrasts radically with surface charging: the electrons involved are much more energetic; their origin is different, both spatially and temporally; the fluxes are relatively small, but the charge buildup can take many hours or days because there can be no neutralization from space plasma or photoemission. Surface properties are immaterial to the IDC process, but the surface potential can influence the internal electric field.

The quantitative determinations of threshold fluence and spectral hardness are dependent upon a number of assumptions, but the results are consistent with laboratory measurements and theoretical models, they are also in agreement with data from CRRES. A directed energy fluence exceeding 1×10^{11} MeV cm⁻², penetrating less than about 0.2 mm of aluminum equivalent, appears to be the cause of the discharges. Using 2-day fluence, measured at satellites

displaced in longitude and local time, has proved satisfactory. This suggests that the corresponding variations are of second order in importance. There is clear evidence that the sensitive circuits have exhibited an increased susceptibility during the mission.

It is stressed that the AME anomalies are not in themselves a threat to the DRA δ mission, but they do provide evidence for the possibility of more serious problems being encountered on GEO spacecraft. There is a clear risk involved when dielectrics (coaxial cables, PCBs, embedded floating conductors) are located outside the spacecraft structure, with less shielding than 1.5 mm of Al. If this cannot be avoided, designers can select leaky dielectrics and desensitize vulnerable circuits; it is a big mistake to strive for unnecessarily fast elements rather than tailoring the response time to the real need. The alternative of additional shielding could be expensive, unless prospective discharge sites can be identified and properly targeted. The AME circuits on DRA ϵ were desensitized by relatively simple measures, which have proved effective.

DRA δ now inadvertently provides an IDC monitor for the GEO environment; this promises to be very useful in the declining phase of the solar cycle. The occurrence frequency of switches, no more than a few a month, reflects a situation that can be contained. However, a single uncontrolled discharge always has the potential for causing serious damage, and the demise of the ANIKs obviously bears witness to that. The results from CRRES, now combined with these statistical data from GEO, present a conclusive explanation for the source of the failures. Spacecraft operations managers should not rest easy until they are sure any such risks have been eliminated. Comparison between ANIK and DRA δ might suggest that the higher the threshold, the fewer the discharges, but that when one does occur it will be larger and much more damaging; the chance of this happening increases with mission duration.

Prompt and open reporting offers the opportunity to learn from others' mistakes. Sometimes the lesson can be fairly inexpensive; Telesat Canada were not so fortunate.

Acknowledgments

This work depends upon data that have been acquired from a number of sources. Thanks are sincerely offered to the following collaborators: Joe Hirman, Dave Speich, and Gayle Nelson, SESC; Joe Allen and Dan Wilkinson, NGDC; Andrew Coates, Nick Flowers, and Sarah Szita, Mullard Space Science Laboratory, University College London; David Gorney and Mike Redding, Aerospace; Keith Derbyshire and Eamonn Daly, ESTEC. Special thanks are due to José and the operations team who made available the crucial anomaly listings.

References

- ¹Anon., "ANIK E2 Disabled," *Aviation Week & Space Technology*, Jan. 31, 1994, p. 28.
- ²Anon., "Telesat Starts ANIK E2 Rescue Effort," *Aviation Week & Space Technology*, Feb. 7, 1994, p. 58.
- ³Garrett, H. B., "The Charging of Spacecraft Surfaces," *Reviews of Geophysics and Space Physics*, Vol. 19, No. 4, 1981, pp. 577-616.
- ⁴Wrenn, G. L., and Sims, A. J., "Surface Charging of Spacecraft in Geosynchronous Orbit," *The Behavior of Systems in the Space Environment*, edited by R. N. DeWitt, D. P. Duston, and A. K. Hyder, Kluwer, Dordrecht, The Netherlands, 1993, pp. 491-511.
- ⁵Robinson, P. A., Jr., "Spacecraft Environmental Anomalies Handbook," Report GL-TR-89-0222, Hanscomb AFB, MA, Aug. 1989.
- ⁶Wrenn, G. L., "Spacecraft Charging Effects," *Solar-Terrestrial Predictions: Proceedings of a Workshop at Leura, Australia*, U.S. Department of Commerce, 1990, pp. 196-205.
- ⁷Vampola, A. L., "Thick Dielectric Charging on High Altitude Spacecraft," *The Aerospace Environment at High Altitudes and Its Implications for Spacecraft Charging and Communications*, CP406, AGARD, May 1987, pp. 28-1-28-7.
- ⁸Robinson, P. A., Jr., and Coakley, P., "Spacecraft Charging—Progress in the Study of Dielectrics and Plasmas," *IEEE Transactions on Electrical Insulation*, Vol. 27, No. 5, 1992, pp. 944-960.
- ⁹Romero, M., and Levy, L., "Internal Charging and Secondary Effects," *The Behavior of Systems in the Space Environment*, edited by R. N. DeWitt, D. P. Duston, and A. K. Hyder, Kluwer, Dordrecht, The Netherlands, 1993, pp. 565-580.
- ¹⁰Allen, J. H., and Wilkinson, D. C., "NGDC Satellite Anomaly Base and Solar-Terrestrial Activity," *Proceedings of IFAC Workshop*, Paris, Dec. 1986, pp. 93-119.
- ¹¹Capart, J. J., and Dumesnil, J. J., "The Electrostatic-Discharge Phenomena on Marecs-A," *ESA Bulletin*, Vol. 34, 1983, pp. 22-27.
- ¹²Rostoker, G., "Geomagnetic Indices," *Reviews of Geophysics and Space Physics*, Vol. 10, 1972, pp. 935-950.
- ¹³Rosen, A. (ed.), *Spacecraft Charging by Magnetospheric Plasmas*, AIAA Progress in Astronautics and Aeronautics, Vol. 47, AIAA, New York, 1976.
- ¹⁴Frederickson, A. R., "Radiation Induced Dielectric Charging," *Space Systems and Their Interactions with Earth's Space Environment*, edited by H. B. Garrett and C. P. Pike, AIAA, New York, 1980, pp. 386-412.
- ¹⁵Beers, B. L., "Radiation Induced Signals on Cables—II," *IEEE Transactions on Nuclear Science*, Vol. NS-24, No. 6, 1977, pp. 2429-2434.
- ¹⁶Wenaas, E. P., Treadaway, M. J., Flanagan, T. M., Mallon, C. E., and Denson, R., "High-Energy Electron Induced Discharges in Printed Circuit Boards," *IEEE Transactions on Nuclear Science*, Vol. NS-26, No. 6, 1979, pp. 5152-5161.
- ¹⁷Koons, H. C., and Gorney, D. J., "Relationship Between Electrostatic Discharges on Spacecraft P78-2 and the Electron Environment," *Journal of Spacecraft and Rockets*, Vol. 28, No. 6, 1991, pp. 683-688.
- ¹⁸Baker, D. N., Blake, J. B., Klebesadel, R. W., and Higbie, P. R., "Highly Relativistic Electrons in the Earth's Outer Magnetosphere 1. Lifetimes and Temporal History 1979-1984," *Journal of Geophysical Research*, Vol. 91, No. A4, 1986, pp. 4265-4276.
- ¹⁹Koons, H. C., and Gorney, D. J., "A Neural Network Model of the Relativistic Electron Flux at Geosynchronous Orbit," *Journal of Geophysical Research*, Vol. 96, No. A4, 1991, pp. 5549-5556.
- ²⁰Coates, A. J., Johnstone, A. D., Rodgers, D. J., Wrenn, G. L., and Sims, A. J., "Quest for the Source of Meteosat Anomalies," *Proceedings of the Spacecraft Charging Technology Conference*, NPS Monterey, 1989, pp. 120-146.
- ²¹Rodgers, D. J., "Correlation of Meteosat-3 Anomalies with Data from the Spacecraft Environment Monitor," European Space Agency, E.W.P. 1620, Noordwijk, The Netherlands, June 1991.
- ²²Daughtridge, S., Garrett, H. B., and Whittlesley, A., "Environment-Induced Anomalies on the TDRS and the Role of Spacecraft Charging," *Journal of Spacecraft and Rockets*, Vol. 28, No. 3, 1991, pp. 324-329.
- ²³Brautigam, D. H., Gussenhoven, M. S., and Mullen, E. G., "Quasi-Static Model of Outer Zone Electrons," *IEEE Transactions on Nuclear Science*, Vol. 39, No. 6, 1992, pp. 1797-1803.
- ²⁴Frederickson, A. R., Holeman, E. G., and Mullen, E. G., "Characteristics of Spontaneous Electrical Discharging of Various Insulators in Space Radiations," *IEEE Transactions on Nuclear Science*, Vol. 39, No. 6, 1992, pp. 1773-1782.
- ²⁵Violet, M. D., and Frederickson, A. R., "Spacecraft Anomalies on the CRRES Satellite Correlated with the environment and insulator samples," *IEEE Transactions on Nuclear Science*, Vol. 40, No. 6, 1993, pp. 1512-1520.
- ²⁶Seltzer, S., "SHIELDSE: A Computer Code for Space-Shielding Radiation Dose Calculations," National Bureau of Standards, TN 1116, May 1980.
- ²⁷Baker, D. N., Higbie, P. R., Belian, R. D., Aiello, W. P., Hones, E. W., Tech, E. R., Halbig, M. F., Payne, J. B., Robinson, R., and Kedge, S., "The Los Alamos Geostationary Orbit Synoptic Data Set," Los Alamos National Lab., LA-8843, Los Alamos, NM, Aug. 1981.
- ²⁸Gorney, D. J., "Final Report of Bulk Charging Study," Aerospace Corp., El Segundo, CA, Sept. 1992.
- ²⁹Shea, M. A., Smart, D. F., Allen, J. H., and Wilkinson, D. C., "Spacecraft Problems in Association with Episodes of Intense Solar Activity and Related Terrestrial Phenomena During March 1991," *IEEE Transactions on Nuclear Science*, Vol. 39, No. 6, 1992, pp. 1754-1760.
- ³⁰Halbleib, J. A., Kensek, R. P., Valdez, G. D., Seltzer, S. M., and Berger, M. J., "ITS: The Integrated TIGER Series of Electron/Photon Transport Codes Version 3.0," *IEEE Transactions on Nuclear Science*, Vol. 39, No. 4, 1992, pp. 1025-1030.
- ³¹Baker, D. N., Goldberg, R. A., Herrero, F. A., Blake, J. B., and Calis, L. B., "Satellite and Rocket Studies of Relativistic Electrons and Their Influence on the Middle Atmosphere," *Journal of Atmospheric and Terrestrial Physics*, Vol. 55, No. 13, 1993, pp. 1619-1628.

H. H. Anderson
Associate Editor